Thermophysical Characterization of Commercial Paper by Laser Infrared Radiometry

A. MANDELIS, M. NESTOROS, A. OTHONOS and C. CHRISTOFIDES

Laser-induced, frequency-scanned infrared photothermal radiometry (PTR) was used successfully in a noncontacting manner to characterize commercial-quality xerographic paper, which was impossible to characterize optically because of its large optical scattering coefficient. A theoretical photothermal model was developed and applied to the frequency-domain data, thus yielding simultaneous measurements of the thermophysical properties (thermal diffusivity and conductivity) of as-received and xerographically processed sheets of paper.

INTRODUCTION

Infrared photothermal radiometry (PTR) has been established as a nondestructive evaluation technique for many classes of solid materials [1,2]. This technique relies on the monitoring of modulated thermal radiation (usually by a laser) from an optically excited surface of a material, which has, at least partially, absorbed the incident radiation and converted it into heat [3]. Generally speaking, a major advantage of photothermal techniques over purely optical methods is their ability to usually yield reliable measurements frequently of either optical and/or thermal parameters of condensed phases, which otherwise may be efficient light scatterers, thus preventing their characterization through conventional optical means [4]. PTR has the additional advantage of detecting photothermal signals remotely and in a noncontacting manner, through collection of the emitted modulated black-body radiation by a fast infrared detector. Therefore, it is suited optimally for on-line diagnostics of industrial materials that exhibit high optical scattering coefficients, such as pulp and paper products.

In this work, the theoretical physical origins of the laser-induced PTR signal from a paper sheet will be presented, and the theory will be applied to as-received, commercially available white xerographic-grade paper and to the same paper processed through a xerographic machine.

JPPS

A. Mandelis*, M. Nestoros,
A. Othonos and C. Christofides
Dept. Natural Sciences
Univ. Cyprus
P.O. Box 537
CY-1678 Nicosia, Cyprus
* On leave from:
Photothermal and
Optoelectronic Laboratories
Dept. Mechan. Indus. Engin.
Univ. Toronto
Toronto, ON, Canada
M5S 3G8

THEORETICAL

The physical basis of infrared photothermal radiometry (PTR) was established early on by Nordal and Kanstad [5,6]. Santos and Miranda [7] presented one-dimensional mathematical models of the PTR signal in both frequency- and time-domains from free-standing solids in air under the assumption of infrared opacity, so that only the surface radiates. Tom et al. [3] extended this theory to include solids in air surroundings, which are not opaque to thermal radiation. Although their work represents a complete solution to the PTR problem with convective heat transfer included, the resulting equations are far too cumbersome for one to follow their physical significance, as they include effects of self-absorption and self-heating of the sample by the radiative heat source. These same authors have established that the radiative heat source is not important for the determination of the temperature fluctuations in PTR and may be neglected [3]. Recently, MacCormack et al. have shown that the convective part of the interfacial heat transfer coefficient is quite small at solid–gas interfaces heated optically by modulated laser sources and may also be neglected [8]. Furthermore, Tom et al. [3] do not address the issue of the presence of an absorbing surface layer, which is the case with a sheet of paper that has gone through the xerographic process.

Therefore, it became necessary to consider the simplified one-dimensional photothermal problem of a free-standing sheet of paper in air, without the effects of convection and reabsorption, which may also have an opaque surface layer of infinitesimal thickness compared to the thickness of the sheet or the thermal diffusion length in the sample. The geometry of the theoretical model is shown in Fig. 1. A free-standing sheet of paper of thickness L, thermal diffusivity α_s, and thermal conductivity k_s, is irradiated with a sinusoidally modulated laser beam of intensity I_o and angular frequency ω. The optical constants β_s and β_{IR} shown in Fig. 1 are meant to be (generally unknown) combinations of the optical absorption and scattering coefficients at, respectively, the excitation wavelength and at the infrared emission wavelength passband collected by the infrared detector optics. A surface-originating thin layer of unknown thickness is assumed to have mean absorptance Q (= surface absorption coefficient × effective layer thickness). This layer represents any changes to the surface optical properties that might ensue following mechanical or thermal processing of the paper. For nonelectronic materials, there is no extraneous modulation of the *IR* emissivity of

the surface other than the emission modulation due to the change in the temperature of the material. For detection in the transmission mode, where the infrared detector is at the other side of the sample, the transmission radiometric signal is [9]

$$S_T(\omega) = K\beta_{IR} \int_0^L e^{-\beta_{IR}(L-x)} \Delta T_s(x,\omega)\,dx \quad (1)$$

where K is an instrumental constant depending on geometrical factors, on the emissivity averaged over the spectral bandwidth of the detector, and on the Stefan-Boltzmann constant. In Eq. (1), $\Delta T_s(x,\omega)$ is the thermal-wave field at a depth x in the bulk of the sample.

The determination of $\Delta T_s(x,\omega)$ can be done by considering the thermal-wave system of equations [10]

$$\frac{d^2\Delta T_j(x,\omega)}{dx^2} - \sigma_j^2 \Delta T_j(x,\omega) = 0 \quad (2)$$

where $j = g$ (gas; air) or s (sample); σ_j is the complex thermal wavenumber defined as

$$\sigma_j = (1+i)\sqrt{\frac{\omega}{2\alpha_j}} \quad (3)$$

and α_j, is the thermal diffusivity of material region (j). There are three equations involved in Eq. (2) with solutions in terms of simple exponential dependence on the spatial coordinate. Specifically for the sample region, the solution takes the form

$$\Delta T_s(x,\omega) = C_1 e^{-\sigma_s x} + C_2 e^{\sigma_s x} - A(\omega)e^{-\beta_s x}$$
$$0 \le x \le L \quad (4)$$

where C_1, C_2 are integration constants and $A(\omega)$ is given by

$$A(\omega) = \frac{I_0\beta_s}{2k_s(\beta_s^2 - \sigma_s^2)} e^{-Q} \quad (5)$$

The integration constants of Eq. (4) can be determined uniquely via the boundary conditions of temperature, ΔT_j, continuity, and heat-flux, $k_j\, d\Delta T_j/dx$, and conservation at the interfaces 0 and L. Especially at the irradiated surface $x = 0$, heat-flux conservation gives

$$-k_s \frac{d\Delta T_s}{dx} + k_g \frac{d\Delta T_g}{dx} = \frac{1}{2} I_0\left(1 - e^{-Q}\right) \quad (6)$$

After some algebraic manipulation of Eqs. (4–6), the values of the integration constants C_1 and C_2 are obtained as shown in Eqs. (7) and (8). In these equations, the following definitions were made

$$b_{gs} \equiv \frac{k_g\sqrt{\alpha_s}}{k_s\sqrt{\alpha_g}}$$
$$r_s \equiv \frac{\beta_s}{\sigma_s} \quad (9)$$

Finally, upon performing the integration in Eq. (1), using Eqs. (4–9) gives the desired expression for the frequency-dependent infrared radiometric transmission signal as shown in Eq. (10).

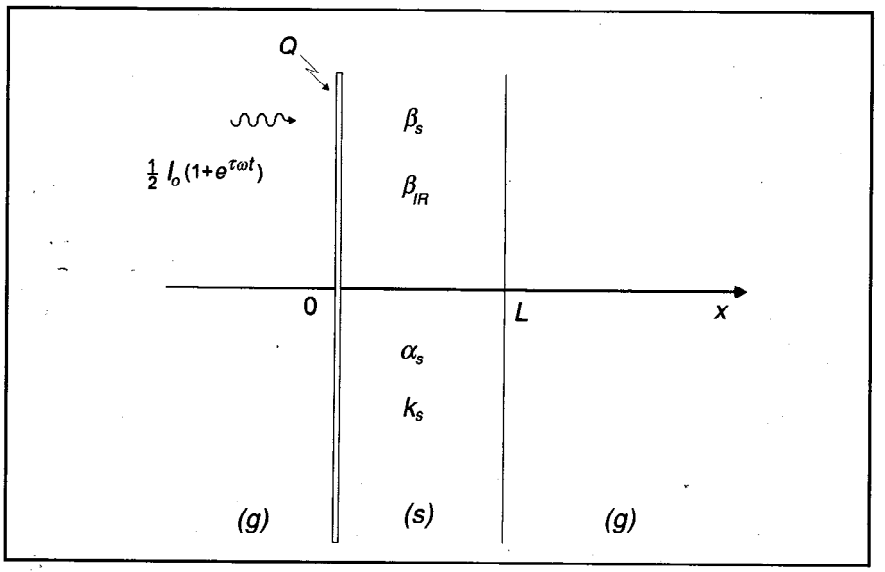

Fig. 1. Schematic of one-dimensional geometry for infrared PTR of a sheet of paper. (*g*): gas (air), and (*s*): solid layer of thickness *L*, thermal diffusivity α_s, thermal conductivity k_s, and effective optical absorption/scattering coefficient β_s (visible) and β_{IR} (infrared). The incident visible-range laser radiation ∿∿→ has intensity I_o and modulation frequency $\omega = 2\pi f$. The surface of the paper sheet may have a thin black layer of infused toner of absorptance *Q*.

EXPERIMENTAL AND RESULTS

Figure 2 shows the PTR experimental set-up used to perform frequency scans of sheet paper samples: a continuous-wave (CW) Ar-Kr laser from Coherent (Innova 70) emitting at mixed 488 and 514.5 nm was used as an unfocused pump beam of spot size ~4 mm, with output power on the order of 100 mW. The intensity of the laser was modulated harmonically using an external sine-wave pulse generator to drive the acousto-optic modulator and to change automatically the modulation frequency applied to it. The frequency scan was in the range 2–1000 Hz, consistent with the thermal energy transport rates across the paper samples studied in this work. Two Ag-

Equation (7)

$$C_1 = \frac{1}{\left[\left(1+b_{gs}\right)^2 e^{\sigma_s L} - \left(1-b_{gs}\right)^2 e^{-\sigma_s L}\right]} \times \left[A\left[\left(1-b_{gs}\right)\left(b_{gs}-r_s\right)e^{-\beta_s L} + \left(1+b_{gs}\right)\left(b_{gs}+r_s\right)e^{\sigma_s L}\right] + \frac{I_0\left(1+b_{gs}\right)\left(1-e^{-Q}\right)}{2k_s\sigma_s} e^{-\sigma_s L}\right]$$

Equation (8)

$$C_2 = \frac{1}{\left[\left(1+b_{gs}\right)^2 e^{\sigma_s L} - \left(1-b_{gs}\right)^2 e^{-\sigma_s L}\right]} \times \left[A\left[\left(1+b_{gs}\right)\left(b_{gs}-r_s\right)e^{-\beta_s L} + \left(1-b_{gs}\right)\left(b_{gs}+r_s\right)e^{\sigma_s L}\right] + \frac{I_0\left(1-b_{gs}\right)\left(1-e^{-Q}\right)}{2k_s\sigma_s} e^{-\sigma_s L}\right]$$

Equation (10)

$$S_T(\omega) = K\beta_{IR}\left[C_1\left(\frac{-\sigma_s L}{\beta_{IR} - \sigma_s}\right) + C_2\left(\frac{\sigma_s L}{\beta_{IR} + \sigma_s}\right) - \left(\frac{C_1}{\beta_{IR} - \sigma_s} + \frac{C_2}{\beta_{IR} + \sigma_s}\right)e^{-\beta_{IR} L} - A\left(\frac{e^{-\beta_s L} - e^{-\beta_{IR} L}}{\beta_{IR} - \beta_s}\right)\right]$$

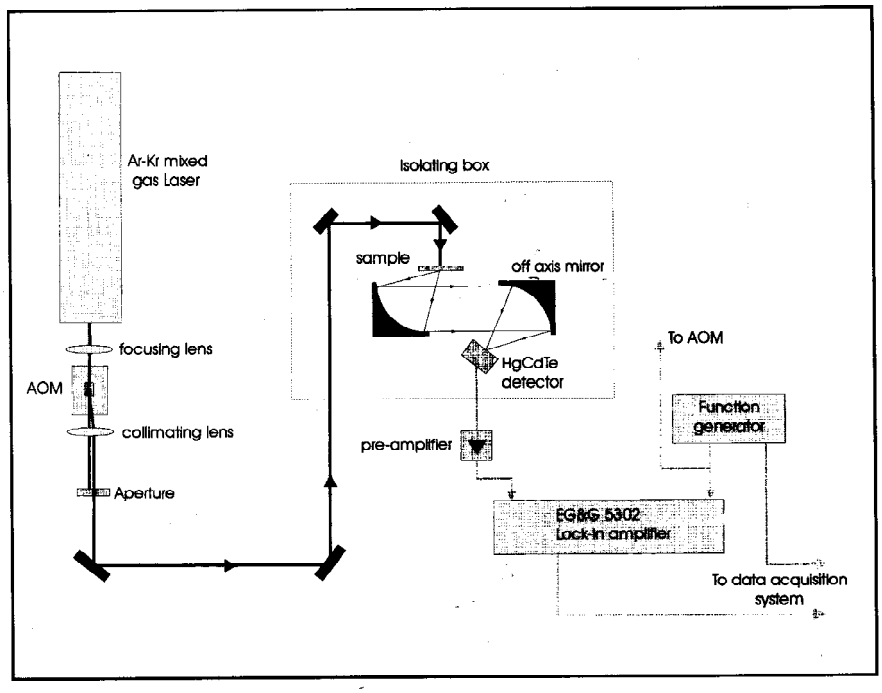

Fig. 2. Experimental set-up for transmission, frequency-scanned PTR. AOM: acousto-optic modulator. The infrared detector was an EG&G Judson J15–D12HgCdTe detector fitted with a Ge window.

coated off-axis paraboloidal mirrors were used to capture and collimate the infrared radiation and, subsequently, to focus it on the active area of a liquid-nitrogen-cooled mercury-cadmium-telluride (MCT: HgCdTe) detector/preamplifier circuit with frequency bandwidth between dc and 1 MHz. The detector was fitted with a Ge window, which filtered out the excitation beam. The spectral response of the detector was in the 2 to 12 μm range. The PTR signal from the preamplifier (EG&G Judson Model PA-350) was fed into the lock-in analyzer (EG&G Model 5302).

This set-up allowed for computer-controlled, automatic frequency scans of the acousto-optically modulated laser intensity. The amplitudes and phases of the PTR signals were stored in the computer for theoretical analysis and calculations. Normalized amplitude and phase curves were further obtained by dividing the former by the respective signal amplitude, and subtracting from the latter the respective signal phase from a thick ("semi-infinite") piece of steel acting as a reference sample. This procedure also takes into account instrument frequency dependencies. Pieces cut from

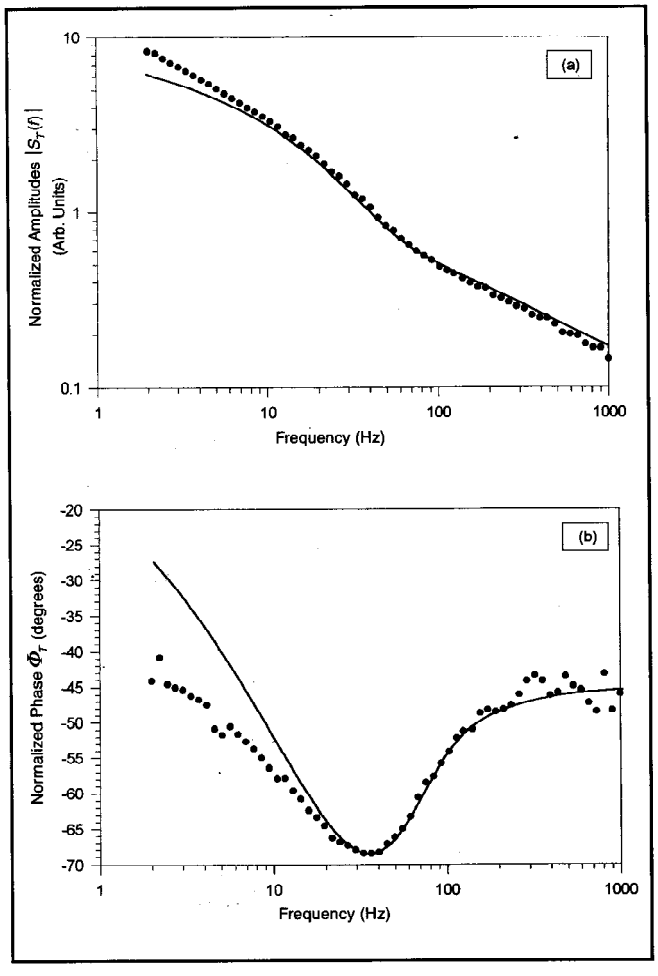

Fig. 3. (a) Normalized amplitude and (b) normalized phase of frequency response of as-received xerographic paper of thickness 78 ± 2 μm. • • •: experimental data; (—): theoretical best-fits to Eq. (10). For best-fit parameter values, see Table I.

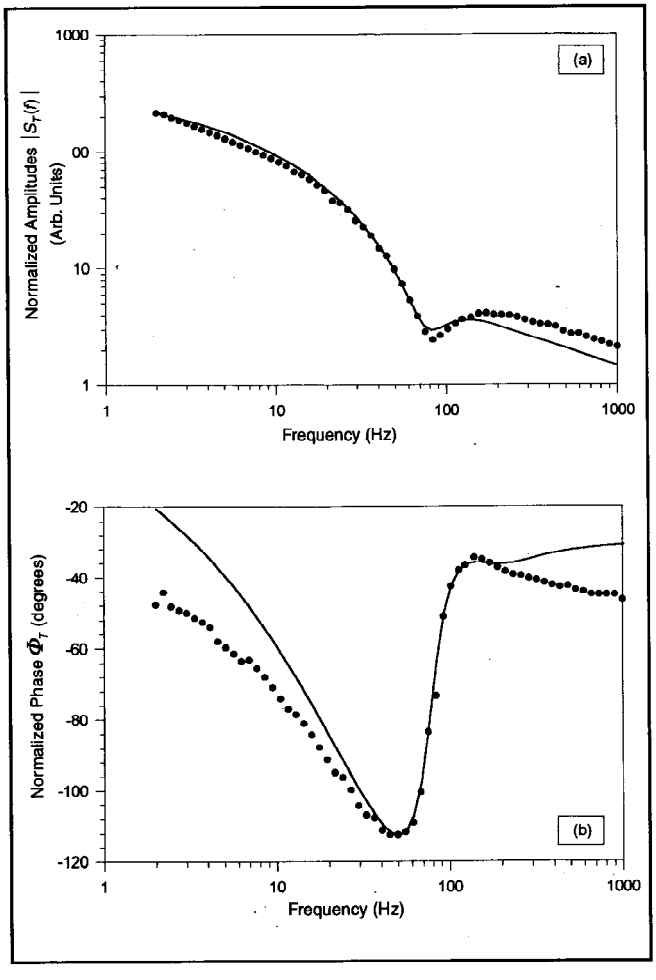

Fig. 4. Similar to Fig. 3 for the same paper after undergoing a complete xerographic cycle, including a thin black toner layer on the surface. The best-fit parameters are shown in Table I.

sheets of standard white xerographic paper of measured thickness 78 ± 2 μm were used for optical transmission, Fourier-transform infrared (FTIR), and PTR experiments. For the optical and the PTR transmission tests, the acousto-optically modulated Ar–Kr laser beam was incident normal to the surface and a sensitive photodiode (or an MCT detector) was placed on the other side of the paper sample, respectively.

Unfortunately, no signal could be detected from the optical transmission experiments because of the large scatter of the light across the body of the paper. Similarly, largely irreproducible results were obtained from the FTIR transmission and backscattering experiments that were performed using a standard FTIR spectrophotometer. It is conceivable that a stronger infrared source might yield reproducibly measurable backscattered signals, based on the throughput (Jacquinot's) advantage of FTIR spectrophotometry. The PTR signals, however, were stable and reproducible. Frequency scans were performed with white paper as received and after one null photocopying cycle. (This sample was the white photocopy of a white original paper.) The results from both samples were similar. Typical PTR responses are shown in Fig. 3. Figure 4 shows similar results obtained with the paper that went through a photocopying cycle using a black original. As a result, a thin black toner layer was formed on the surface. Typical acquisition times for the foregoing frequency scans were ~15–20 min/scan. This rate can be reduced by approximately a factor of 1000 using signal cross-correlation and spectral analysis techniques. The statistics of the PTR signals from the same site and from different sites on a single paper sample sheet were very similar and reproducible with signal variations of less than 5% through the entire frequency range of Figs. 3 and 4. Signal variations of less than 7% between paper sheets by the same manufacturer were observed.

THEORETICAL FITS TO THE DATA AND DISCUSSION

The theoretical curves superposed on the data of Figs. 3 and 4 were obtained following a trial and error procedure for optimally fitting Eq. (10). It can be seen from Eq (10) that the fit is a multivariable one involving four parameters: α_s, k_s, β_s, and β_{IR}. The value of the surface absorptance was set to $Q = 0$ for the white paper, whereas it was allowed to vary for the sample with the black surface layer. Therefore, this sample involved a five-parameter fit. Unfortunately, no independent measurements of at least the optical parameters were available, as no reproducible optical parameter measurements could be made with our optical experiments. Therefore, the simultaneous variation of all four (or five) parameters toward a best fit raised the issue of the uniqueness of the fit. Even though there can be no rigorous proof of the uniqueness of the calculated best-fit set of parameters, the requirement for the theory to yield acceptable fits to both amplitude and phase data, plus the fact that both types of paper in Figs. 3 and 4 originated from the same substrate sample, proved to yield stringent enough constraints to raise the level of confidence in the uniqueness of the sets of calculated parameters. The values of the optical and thermophysical parameters for our paper samples are shown in Table I. For the calculation of the thermal coupling coefficient b_{gs}, the literature values [11] for air were used: $k_g = 2.38 \times 10^{-2}$ W/mK and $\alpha_g = 0.2 \times 10^{-4}$ m^{-4} m^2/s.

TABLE I
THERMOPHYSICAL AND OPTICAL BEST-FIT PARAMETER VALUES FOR COMMERCIAL XEROGRAPHIC PAPER

	α_s ($\times 10^{-6}$ m^2/s)	k_s ($\times 10^{-6}$ W/mK)	β_s ($\times 10^4$ m^{-1})	β_{IR} ($\times 10^4$ m^{-1})	Q
As-received/null photocopy	4.6	100	4.8	7.5	0
With black photocopied layer	5.5	100	4.8	8.5	1.7

When independent theoretical fits to either amplitude or phase of the PTR signal were attempted, several widely different sets of the parameters could be found, giving excellent fits to the data. Under the constraint of fitting both signal channels, the only sets of parameters capable of giving acceptable (but not excellent) fits were those in Figs. 3 and 4 and in Table I. Tolerance to parameter variations depended on the particular parameter: the position of the minimum in the phase (Figs. 3,4), of the local amplitude minimum (Fig. 4), and of the change in the sign of the curvature in the amplitude of Fig. 3, depend most sensitively on the values of the thermal diffusivity and conductivity. Physically, these extrema are the result of thermal standing-wave interference in the bulk of the paper sample and, as such, they depend strongly on the thickness and the thermal diffusivity [12]. They also depend more weakly on the thermal coupling coefficient, b_{gs}, at the solid–gas interface [12]. Therefore, varying these thermophysical parameters to match the extrema could be done without having to consider changes in the optical properties. The values of β_s and β_{IR} obtained through fits of the theory to the experimental data have only been considered as characteristic of a given sheet of paper, which may vary substantially with time, ambient conditions, exposure to light, etc. On the other hand, the values of thermophysical parameters measured by transmission PTR represent bulk conditions in the paper, and are considered to be insensitive relatively to surface conditions [8,10]. It is the value of the thermal diffusivity that characterizes the bulk (thickness-averaged) quality of a sheet of paper. The quality of the optimum fits in Figs. 3 and 4 varies within a given curve. The low-frequency end of the data could not be fitted well below the minimum of the phases. Furthermore, the paper with black surface layer shows clear disagreement with the theory in the high-frequency thermally thick regime, where $\mu_s(\omega) >> L$.

The low-frequency discrepancies likely are due to the inadequacy of the reference sample to reproduce exactly the one-dimensional transfer function of the instrument. Three-dimensional effects have been observed previously with steel samples below 20 Hz even with laser beam sizes 5 or 10 mm [8]. The paper samples in that same region, however, behaved in an entirely one-dimensional manner because of the very large beam size compared to the sample thickness. The discrepancies observed at the high-frequency range of Fig. 4 are hypothesized to be due to the nonuniformity of the paper sample that underwent the xerographic process. The foregoing hypothesis is also consistent with the values obtained in Table I. The diffusivity of the blackened paper has increased by ~16%, whereas the conductivity has remained constant (all our measurements carry uncertainties up to 4% for the diffusivity and 8% for the conductivity). This may happen only if the specific heat, C_s, and/or the density, ρ_s, decreases, according to the definition of the thermal diffusivity

$$\alpha_s = \frac{k_s}{C_s \rho_s} \tag{11}$$

The most probable event here is a change (decrease) in the density of the paper mass directly below the blackened area, due to the possibly steep increase in the temperature of the near-surface region upon exposure to the xerographic process. The value of $Q = 1.7$ indicates that the black surface layer absorbed $1 - e^{-Q} = 81.7\%$ of the incident radiation. This renders the paper sample almost entirely opaque, localizes the laser heating, and tends to accentuate the presence of thermal inhomogeneities in the near-surface region. Independent verification of the thermophysical property values obtained by use of laser-induced PTR is not easy, since there exists little in terms of measurements of these quantities for paper, to the authors' best knowledge. Touloukian et al. [13] have published the value $k_s = 4 \times 10^{-2}$ W/mK for the thermal conductivity of rice paper 30 μm thick measured under a load of 144.8 kPa. This value is 40 times higher than those calculated in the present work, but any further comparisons are hard to make.

CONCLUSIONS

1. Laser-induced infrared photothermal radiometry (PTR) was applied for the first time to the measurement of thermophysical properties of commercial xerographic paper sheets. Whereas no reproducible

optical or FTIR signals could be obtained, the PTR technique produced high-quality frequency scans from as-received, as well as photocopied paper with a black surface layer of toner.

2. A theoretical model pertinent directly to the PTR of thin paper sheets was developed and compared with the experimental data. Acceptable to good fits were obtained, which were further optimized and yielded sets of thermophysical and optical parameters for the paper with common origin and different history, as shown in Table I.
3. As a result of this procedure, the thermal diffusivity and conductivity of the paper samples were calculated. The concomitant values of the optical properties (visible and infrared effective absorption constants) were also calculated. Yet, the latter can be used only as reference values, since the physical origins of these optical parameters are not well established (partly due to bulk absorption and scattering, and partly due to variable surface conditions).
4. The implications of the present work as noncontact, nonintrusive diagnostic methodology for the on-line or off-line quality control of industrial pulp and paper products at various stages of the manufacturing cycle, including the final product, are broad, especially in view of the fact that purely optical techniques fail to yield reproducible results due to the highly optically scattering nature of paper.

REFERENCES

1. IMHOF, R.E., ZHANG, B. and BIRCH, J.S., "Photothermal Radiometry for NDE" in Progress in Photothermal and Photoacoustic Science and Technology, Vol. II, A. Mandelis, Ed., Prentice-Hall, Englewood Hts., NJ, 185–236 (1994).
2. TAM, A.C., "Pulsed Laser Photoacoustic and Photothermal Detection" in Photoacoustic and Thermal Wave Phenomena in Semiconductors, A. Mandelis, Ed., North-Holland, New York, Ch. 8 (1987).
3. TOM, R.D., O'HARA, E.P. and BENIN, D., "A Generalized Model of Photothermal Radiometry", *J. Appl. Phys.* 53(8):5392 (1982).
4. MORTERRA, C., LOW, M.J.D. and SEVERDIA, A.G., "Some Effects of Specular and Diffuse Reflection on Infrared Photoacoustic Spectra", *Infrared Phys.* 22:221 (1982).
5. NORDAL, P.-E. and KANSTAD, S.O., "Photothermal Radiometry", *Physica Scripta* 20:659 (1979).
6. NORDAL, P.-E. and KANSTAD, S.O., "Visible-Light Spectroscopy by Photothermal Radiometry Using an Incoherent Source", *Appl. Phys. Lett.* 38:486 (1981).
7. SANTOS, R. and MIRANDA, L., "Theory of the Photothermal Radiometry with Solids", *J. Appl. Phys.* 52(6):4194 (1981).
8. MacCORMACK, E., MANDELIS, A., MUNIDASA, M., FARAHBAKHSH, B. and SANG, H., "Measurements of the Thermal Diffusivity of Aluminum Using Frequency-Scanned, Transient- and Rate-Window Photothermal Radiometry. Theory and Experiment", *Intl. J. Thermophys.* (in press).
9. LEUNG, W.P. and TAM, A.C., "Techniques of Flash Radiometry", *J. Appl. Phys.* 56(1): 153 (1984).
10. MANDELIS, A., McALLISTER, K., CHRISTOFIDES, C. and XENOFONTOS, C., "A Pilot Study in Non-Contact Laser Photothermal Archaeometry of Ancient Statuary Pedestal Stones from Cyprus", *Archaeometry* 37(2):257 (1995).
11. CRC Handbook of Chemistry and Physics, 74th ed., D.R. Lide, Ed., Chemical Rubber, Cleveland, OH, 6–1 and 6–199 (1993).
12. SHEN, J. and MANDELIS, A., "Thermal-Wave Resonator Cavity", *Rev. Sci. Instrum.* 66(10):4999 (1995).
13. TOULOUKIAN, Y.S., POWELL, R.W., HO, C.Y. and KLEMENS, R.Q., "Thermal Conductivity", IFI/Plenum, New York, Specification Table No. 385.1127 (1970).

REFERENCE: MANDELIS, A., NESTOROS, M., OTHONOS, A. and CHRISTOFIDES, C., Thermophysical Characterization of Commercial Paper by Laser Infrared Radiometry. Journal of Pulp and Paper Science, Vol. 23(3) J108–112 March 1997. Paper offered as a contribution to the Journal of Pulp and Paper Science. Not to be reproduced without permission from the Technical Section, CPPA. Manuscript received March 20, 1996; revised manuscript approved for publication by the Review Panel November 19, 1996.

ABSTRACT: Laser-induced, frequency-scanned infrared photothermal radiometry (PTR) was used successfully in a noncontacting manner to characterize commercial-quality xerographic paper, which was impossible to characterize optically because of its large optical scattering coefficient. A theoretical photothermal model was developed and applied to the frequency-domain data, thus yielding simultaneous measurements of the thermophysical properties (thermal diffusivity and conductivity) of as-received and xerographically processed sheets of paper.

RÉSUMÉ: Nous avons utilisé avec succès, en privilégiant un mode d'emploi sans contact, la radiométrie photothermique à l'infrarouge à balayage de fréquence produit par un faisceau laser pour caractériser du papier xérographique de qualité commerciale, lequel était impossible à caractériser optiquement à cause de son coefficient de dispersion optique élevé. Nous avons développé un modèle photothermique théorique et l'avons appliqué aux données relatives aux fréquences. En ce faisant, nous avons mesuré simultanément les propriétés thermophysiques (la conductivité et la diffusité thermiques) des feuilles de papier tel que réceptionnées et les feuilles de papier traitées xérographiquement.

KEYWORDS: XEROCOPY PAPERS, PHYSICAL PROPERTIES, RADIOMETRY, NONDESTRUCTIVE TESTS, THERMAL PROPERTIES, CONTACTLESS MEASUREMENT, LASERS, INFRARED DETECTORS, EVALUATION.